

**Supplementary Information:**

**Coaxial SnO<sub>2</sub>@TiO<sub>2</sub> Nanotube Hybrids: From Robust Assembly Strategies to Potential Application in Li<sup>+</sup> Storage**

Xiaomeng Wu<sup>a</sup>, Shichao Zhang<sup>a</sup>, Lili Wang<sup>a</sup>, Zhijia Du<sup>a</sup>, Hua Fang<sup>a</sup>, Yunhan Ling<sup>b</sup>, Zhaohui Huang<sup>c</sup>

<sup>a</sup>School of Materials Science and Engineering, Beijing University of Aeronautics and Astronautics, Beijing 100083, China

<sup>b</sup>Department of Materials Science and Engineering, Tsinghua University, Beijing 100084, China

<sup>c</sup>School of Materials Science and Technology, China University of Geosciences (Beijing), Beijing 100083, China

Corresponding Authors: csc@buaa.edu.cn

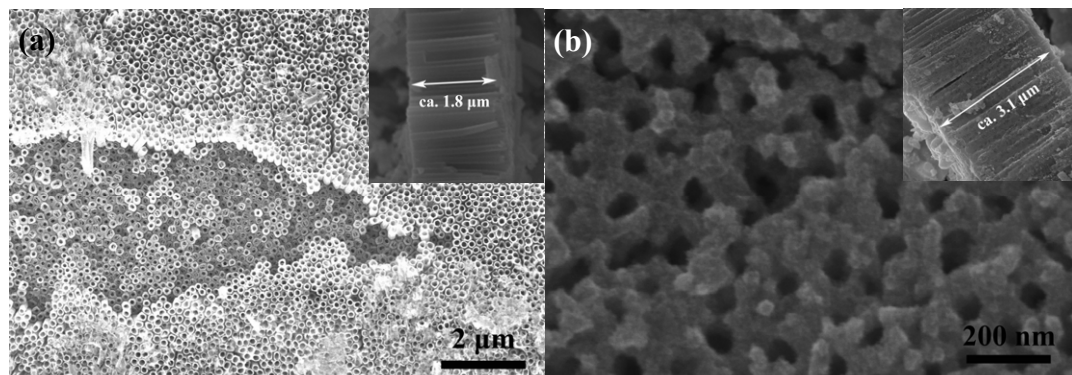


**Fig. S1.** FESEM images of the synthesized coaxial nanotubes array used for Li<sup>+</sup> storage. a) Top- and cross-section (inset) views of coaxial SnO<sub>2</sub>@TiO<sub>2</sub> nanotubes array synthesized with the electrochemical method. b) Top- and cross-section (inset) views of coaxial C/SnO<sub>2</sub>@TiO<sub>2</sub> nanotubes array synthesized with the solvothermal method.

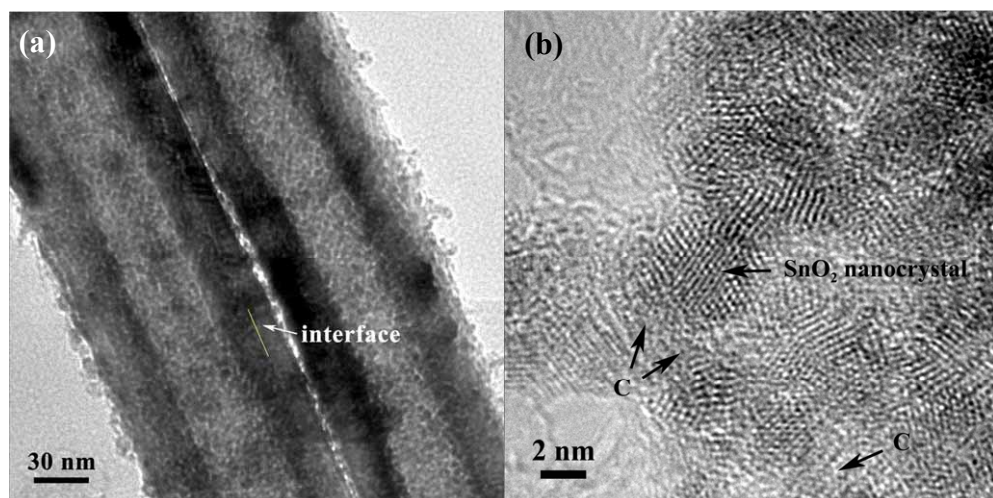


**Fig. S2.** (a) TEM image of the C/SnO<sub>2</sub>@TiO<sub>2</sub> coaxial nanotubes and (b) the HRTEM image of the C/SnO<sub>2</sub> layer at the upper lip region.

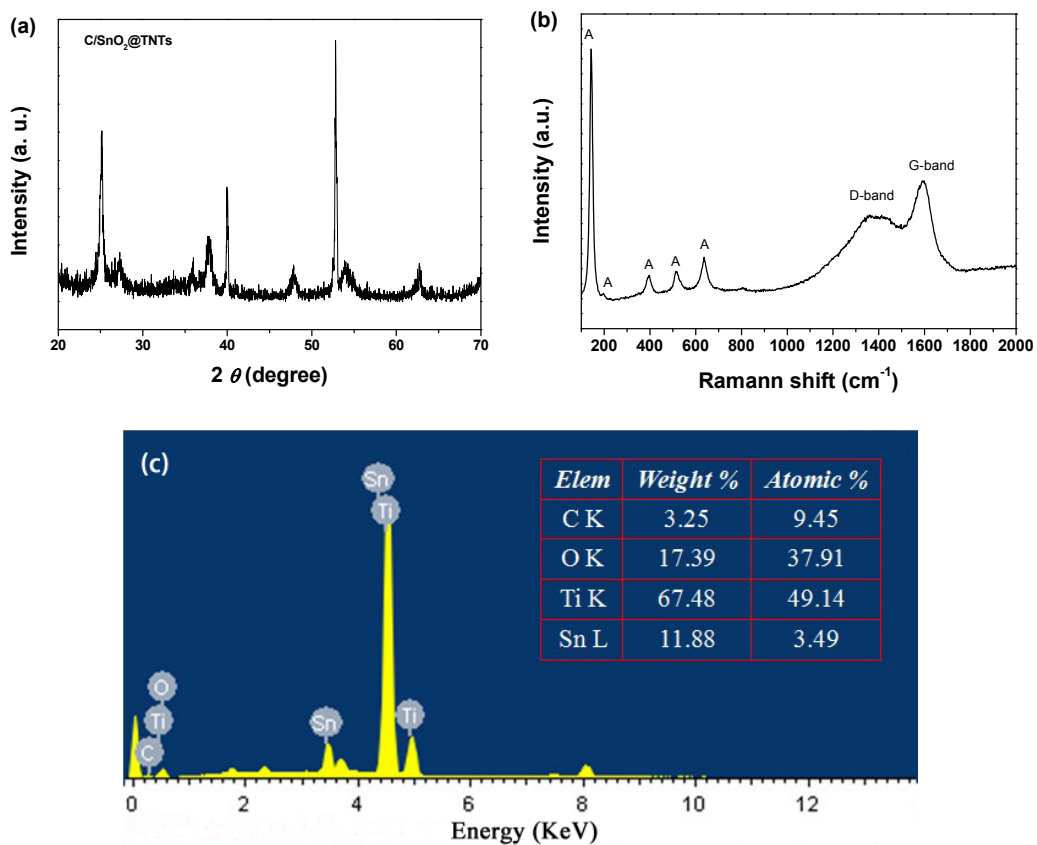


**Fig. S3.** (a) XRD pattern of the coaxial C/SnO<sub>2</sub>@TNTs. (The low content of amorphous carbon in the C/SnO<sub>2</sub>@TNTs brought no diffraction peaks corresponding to graphitic or amorphous carbon were observed in the XRD pattern.) (b) Raman spectrum of C/SnO<sub>2</sub>@TNTs. The results exhibit two kinds of peaks, namely, the graphite carbon peak (G peak) located at ~1597 cm<sup>-1</sup> and the disordered carbon peak (D peak) at ~1341 cm<sup>-1</sup>. Besides, the typical peaks (144, 197, 400, 515, and 640 cm<sup>-1</sup>) corresponding to anatase phase are also appeared. (c) EDS spectra obtained after C/SnO<sub>2</sub>@TNTs scratched from the Ti substrate for eliminating the influence of the substrate.

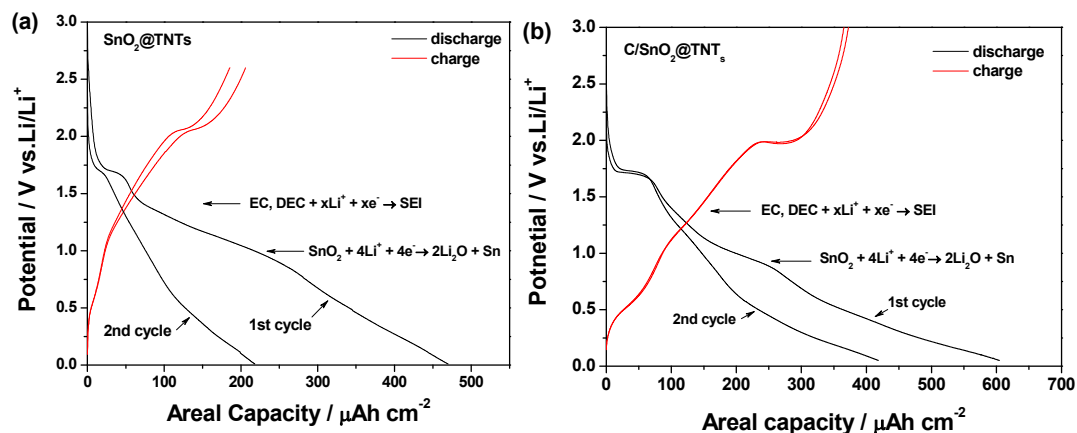


**Fig. S4.** Selected galvanostatic discharge/charge curves of the electrochemically prepared SnO<sub>2</sub>@TNTs (a) and solvothermally prepared C/SnO<sub>2</sub>@TNTs (b), respectively.

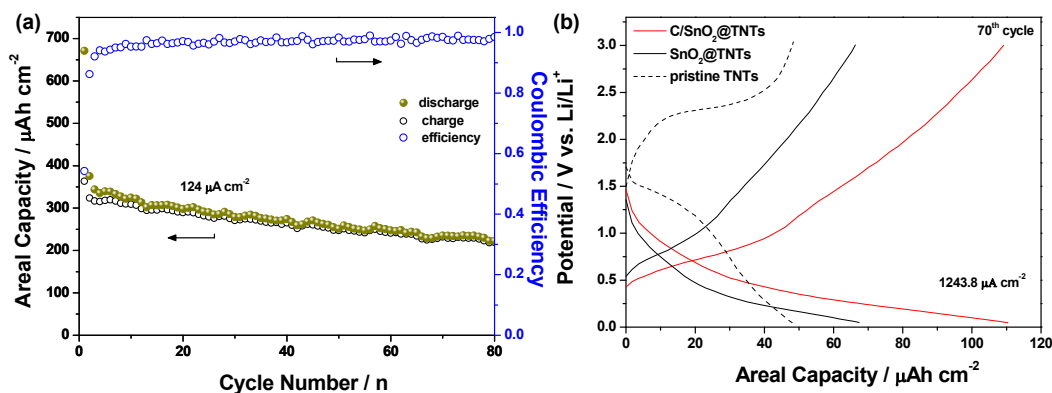


**Fig. S5.** (a) Cycling performance of SnO<sub>2</sub>@TNT<sub>s</sub> cycled at a constant current density of  $\sim 124 \mu\text{A/cm}^2$  and (b) galvanostatic charge-discharge curves for pristine TNTs, SnO<sub>2</sub>@TNTs and C/SnO<sub>2</sub>@TNTs at a current density of  $1240 \mu\text{A/cm}^2$  (the 70th cycle)

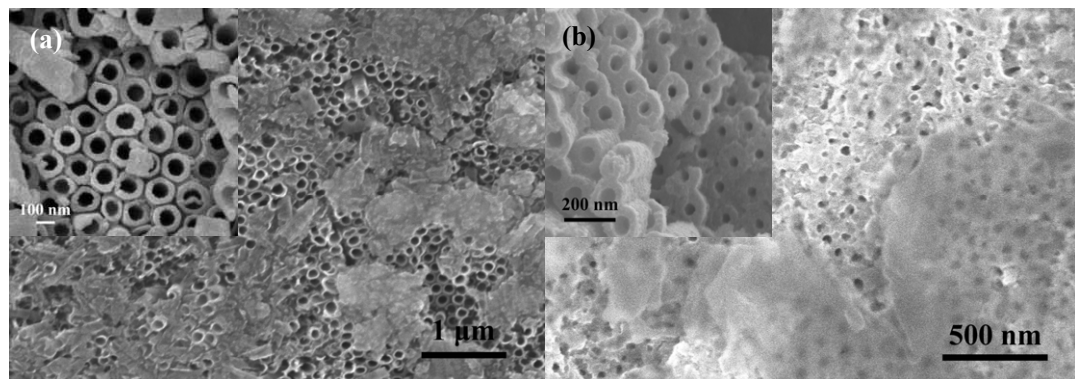


**Fig. S6.** FESEM images after charge/discharge cycles (insets: higher magnification obtained after scratching): (a) Electrochemically prepared SnO<sub>2</sub>@TiO<sub>2</sub> (after 50 cycles); (b) Solvothermally prepared C/SnO<sub>2</sub>@TiO<sub>2</sub> (after 80 cycles).